# Application of digital rock physics for geophysical rock properties

Naum Derzhi*, Carl Sisk (Ingrain Inc.) and Zubair Kalam, (ADCO)



## Abstract

Traditionally,the values of reservoir rock properties have been acquired from log data or direct measurement in a physical laboratory. Recent advances in imaging and image processing, together with improved availability of high performance computing, gave rise to digital techniques for investigating the properties of rock samples. These techniques are based on high-resolution imaging of the rock's pore space, segmentation of the images into pores and various minerals and simulation of the physical processes controlled by the desired rock properties. These techniques form the novel discipline of digital rock physics (DRP). The goal of the current work is to validate the results of DRP measurements of geophysical parameters by comparing them with the results obtained in traditional physical laboratories.

This study includes eight core plugs from a Cretaceous formation, representing four reservoir rock types. Multiple sub-samples of each core plug were taken and analyzed using the digital rock physics technique.
Our DRP computations are compared with the results of physical measurements of the geophysical properties on samples from Cretaceous formations. The latter measurements were conducted on regular core plugs, several cm in size, much larger than the digital rock samples used in this study. Although some of the physical data represent samples from wells different from where the digital samples used here were extracted, these physical samples cover the rock types included in the study. The geophysical property values obtained in the digital rock physics laboratory closely match the results of physical measurements.

## Introduction

Digital Rock Physics (DRP) is a novel way of investigating and estimating the bulk, elastic, electrical and transport properties of porous rocks. In this approach, high-resolution images of the rock's pores and mineral grains are obtained and processed and the rock properties are evaluated by numerical simulation of the physical processes of interest at the pore scale.

Comparisons between the rock properties obtained by DRP studies and those obtained by other means, especially laboratory tests, are important for validating this new technology and using the results it provides with confidence. In this paper we present a comparative study of digital rock physics and laboratory evaluations of the elastic properties of carbonate samples.

## Characterization of the Reservoir Core Samples

The study was conducted on eight 1½" diameter cylindrical core plugs representing four Lower Cretaceous carbonate reservoir rock types ("RRT"), according to a current Abu Dhabi Company for Onshore Operations (ADCO) RRT definition (Grötsch, 1997).This ADCO definition is based mainly on the sample's porosity, permeability and mercury injection capillary pressure measurements. This characterization had also been linked to a standardized ADCO lithofacies description, and assumed environment of deposition (Strohmenger, 2006).

These four RRTs are each described below.

RRT-2:
Samples S9 and S18 are examples of Coated-Grain, Algal, Skeletal Rudstone to Floatstone "CgASR" lithofacies. The "CgASR" lithofacies implies deposition in a shallow subtidal, high-energy open platform above fair weather wave base, upper ramp, near shoal crest.

RRT-3:
Samples 14 and 21 are examples of Skeletal, Peloid Grainstone ("SPG") lithofacies. The SPG lithofacies implies deposition in a shallow subtidal to intertidal, high-energy open platform above fair weather wave base, possibly upper ramp beach, near shoal crest and near inner shoal.

RRT-4:
Samples 1V and 22 are. The SPP lithofacies implies deposition in shallow subtidal to intertidal, moderate-energy restricted and open platform above fair weather wave base, possibly, inner shoal and upper ramp.

RRT-6:
Samples 10V and 33 are examples of Orbitolinid, Skeletal Wackestone (OSW) lithofacies. The OSW lithofacies implies deposition in low-energy, open platform below fair weather wave base, possible middle ramp.

## Laboratory Tests Data

The laboratory test data used in this study were accumulated by ADCO in the course of several years. The tests were performed on cores from the same rock type and formation, but, in most cases, not directly on the cores used in this DRP study. Different samples were used for elastic and electric tests.

*Elastic Moduli*

The samples used in measurements of elastic properties were room dry.

Most laboratory tests were performed at ambient stress conditions. However, a number of measurements had been

performed at varying effective stress conditions up to 44 MPa. The laboratory tests provided values of dynamic elastic moduli, i.e., the compressional and shear wave velocities were measured directly and then the moduli were calculated from these velocity and bulk density values. Each rock type was represented by just one or two samples in the experiments with varying effective stress, which makes it impossible to analyze the trends for each rock type independently. In addition, the sets of effective stress values differed from sample to sample. As a result, the data obtained in laboratory tests at each stress level were treated as a single data set.

*Formation Factor*

The samples used in formation factor measurements were saturated with formation water. The measurements were performed at 2 MPa of confining stress. For each rock type, only one or two samples were available for formation factor comparisons.

**Digital Rock Physics Methods and Data**

In this study elastic parameters and formation factors were obtained from the same samples.

For the purposes of this study, several sub-samples were extracted from each core plug and their pore-scale images were obtained at ambient stress condition using X-Ray Computed Tomography (CT) with resolutions ranging from 100 nano-meters to 40 micro-meters. The images were processed (segmented) to identify locations in the rock occupied by pores and various minerals. The result of this process is a digital rock, i.e., a 3-D matrix of the same size as the CT image where each cell is either a solid, or a pore, and is assigned the elastic moduli accordingly to the mineral or fluid occupying the corresponding location in the rock sample. Since the physical samples were room-dry, the elastic moduli and density of the pore fluid in our computations were zero.

The same 2-D slices of the raw and segmented CT image are shown in Figure 1. In the raw image, different shades of gray correspond to the difference in the X-ray attenuation of the rock: higher X-ray attenuation corresponds to higher CT values, which are displayed as light areas in the image. Segmentation process splits this raw image into three phases: pores (black), solid calcite (white), and micro-porous calcite (gray).

The pores in the micro-porous calcite phase are too small to be visible at the resolution of this scan (about 4 micrometers). The density of this phase is estimated from the difference in the CT values observed in the pores, solid calcite, and micro-porous phase. Its porosity was computed accordingly by assuming that the solid is pure calcite and the micropores are empty. In addition, representative samples of the micro-porous phase had been imaged with high-resolution CT scans (voxel size about 65 nanometers). Analysis of the high-resolution images, including segmentation, confirmed the porosity estimates made from the CT values.

The elastic properties of these rocks were estimated by simulating small elastic deformations in the digital rock using Finite Element Method (FEM) software module based on the code described in (Bohn, 2003). In this method each voxel of the digital rock is treated as an elastic cube with elastic properties defined by its phase code. The method finds the distribution of stresses and strains in the rock by minimizing the energy of elastic deformation, and the rock's dynamic moduli are calculated from the average stresses and strains. The electric properties (formation factor) were estimated by digitally saturating the pore space with conductive fluid, and simulating the electric current throught the sample, using similar software module.

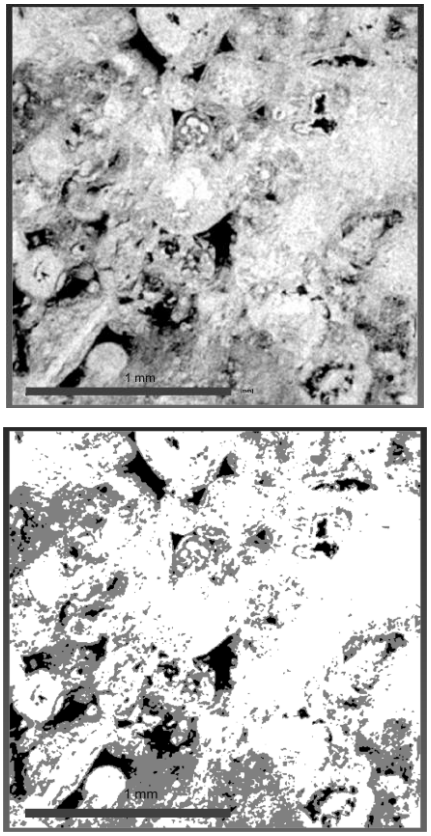


***Fig. 1**. 2D slice of the raw CT image of sample S18 (top) and the same slice segmented into pores, solid calcite, and microporous calcite (bottom).*

As mentioned earlier, for this study the voxels in the pore phase were assigned zero density and moduli. The voxels in the solid calcite phase were assigned the density of 2.71 g/cc, bulk modulus of 76.8 GPa, and shear modulus of 32 GPa. The calcite phase was assigned zero electric conductivity.

The elastic properties of each micro-porous phase were determined based on its average porosity, using the modified upper Hashin-Shtrikman bound model (Mavko et al, 2009). The relevance and accuracy of this model had been confirmed by comparing it with the elastic property values calculated from high-resolution scans (Figure 2). The formation factors of each micro-porous phase were determined by calculating the formation factor on the same scans.

**Comparisons and Discussion**

Since the laboratory tests and DRP measurements were performed on different rock samples, it is impossible to

directly compare DRP with laboratory tests. Instead, we are comparing the trends of the rock properties versus the total porosity.

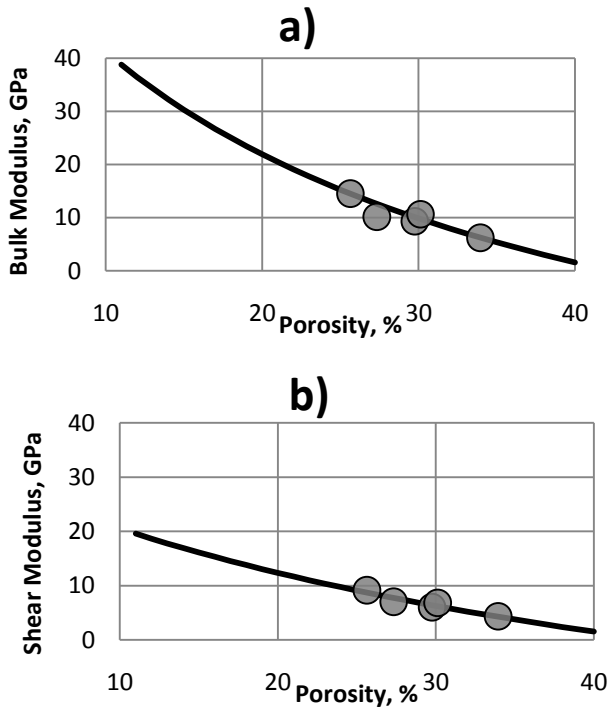


***Fig. 2.*** *Comparison of the model used for assigning the elastic properties of micro-porous phase with calculations performed on selected high-resolution digital rocks representing this phase. a) Bulk modulus; b) Shear modulus. Circles represent values obtained on high-resolution digital rock. Solid lines are from the model as described in the text.*

*Velocities and Dynamic Elastic Moduli*

Comparison of the compressional wave velocity trends between the DRP and the traditional laboratory methods is presented in Figure 3 at different effective pressures. The trends formed by the Vp values obtained by DRP or laboratory tests are similar in shape. The Vp values produced by DRP from rocks imaged at ambient conditions are consistenly higher than those from the laboratory tests at ambient stress conditions, but closely match the Vp values from the laboratory tests performed at 30 MPa effective stress, which is close to the effective stress in the reservoir.

Shear wave velocity (Vs) and dynamic elastic moduli (e.g., Young's modulus) values exhibit a similar behavior.

We conclude that even though the DRP imaging was performed at ambient condition, the DRP results come closer to the laboratory results obtained not at the ambient conditions, but rather at the in-situ effective stress.

This velocity-stress behavior is most likely caused by micro-cracks which appear in the rock fragments unstressed from the in-situ pressure to practically zero stress when they were lifted from the reservoir depth and placed on benchtop. These micro-cracks significantly soften the rock, which results in relatively low elastic wave velocities and dynamic moduli measured at ambient stress condition. Re-applying the stress in the course of laboratory tests causes closure of some of these cracks, resulting in higher velocities, measured at reservoir level effective stress.

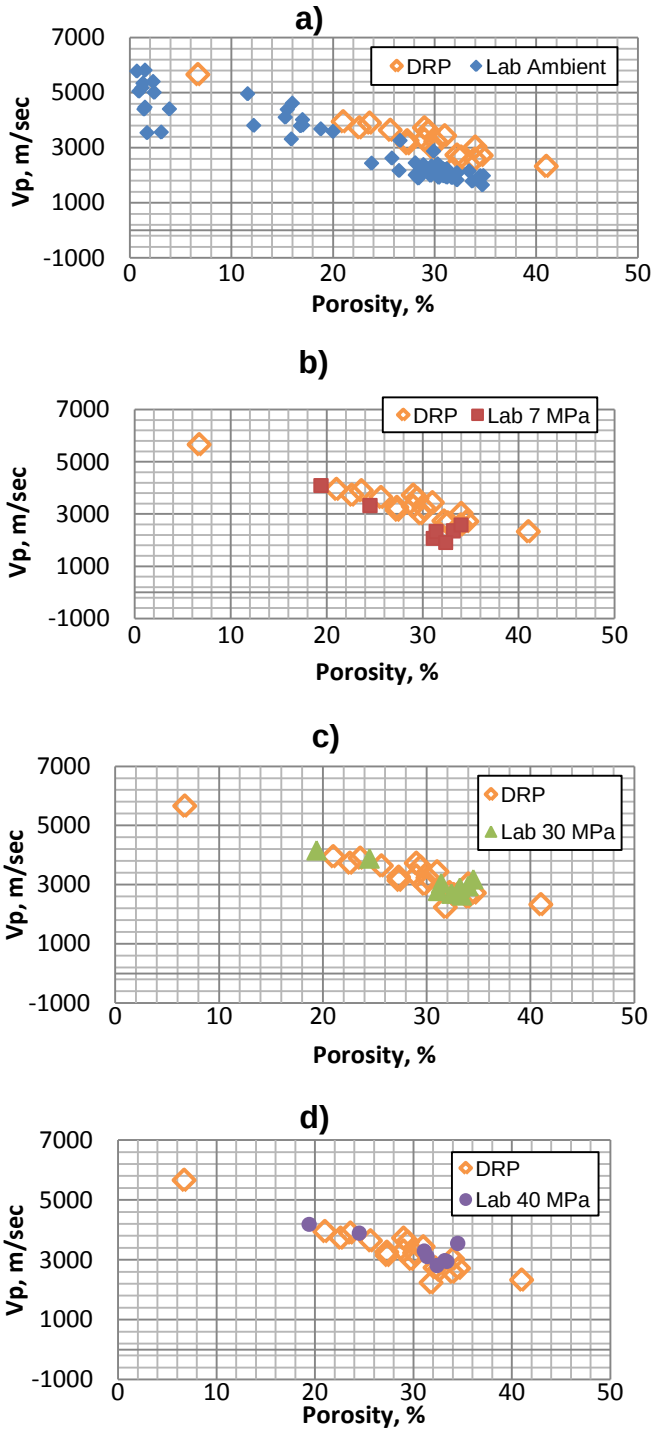


***Fig. 3.*** *Comparison of Vp values obtained in DRP (orange open diamonds) with Vp values from the laboratory tests obtained at ambient conditions (a, blue diamonds), effective stress 7 MPa (b, red squares), effective stress of 30 MPa (c, green triangles), and effective stress 40 MPa (d, purple circles).*

The difference between the digital and physical laboratory is that in the former we compute what we image. This means that if we choose not to image the stress-release cracks, the simulations on the resulting digital rock should properties close to the ones measured under stress – the conditions most relevant to any geophysical application.

Therefore, without an additional effort, the DRP method can provide the elastic property values close to those that would be measured at reservoir stress condition.

*Poisson's Ratio*

The trends of the Poisson's ratio versus porosity obtained from the laboratory tests and DRP are remarkably different (see Figure 5): the DRP values form a consistent trend in agreement with the rock physics models, while the values obtained from the laboratory tests do not form any trend at all. It can be argued, that the Poisson's ratio values provided by DRP can be used with much greater confidence than these laboratory results.

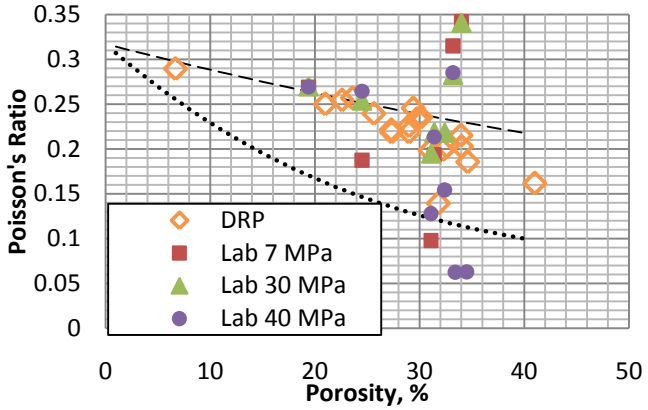


***Fig. 5.*** *Comparison of Poisson's ratio obtained in DRP (orange open diamonds) with values from laboratory tests obtained at effective stress 7 MPa (red squares), effective stress 30 MPa (green triangles), and effective stress 40 MPa (purple circles). The dotted and dashed lines represent Poisson ratio predictions by the differenitial effective medium model with aspect ratios of 0.1 and 0.3 respectively*

*Formation Factor*

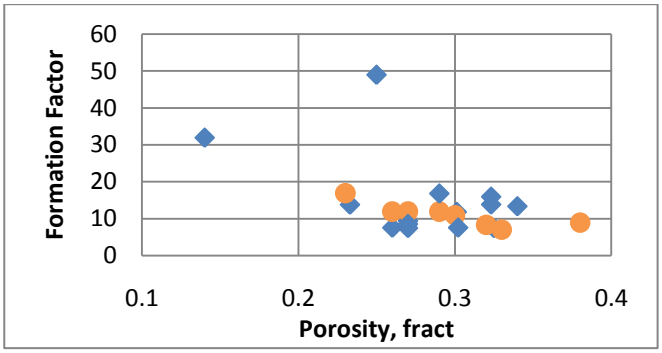


***Fig. 6.*** *Comparison of Formation Factor values obtained in DRP (orange open diamonds) with values from laboratory tests (blue diamonds.Both trends are remarkably similar*

## Conclusions

The use of digital rock physics has been established for a variety of formations and applications through various peer reviewed papers. It is especially important to notice that digital rock physics allows obtaining all geophysical properties on the same rock sample.The application for elastic properties and electrical properties for carbonates has achieved acceptable results.

## Acknowledgments

The authors acknowledge the support of Ingrain, Inc and Abu Dhabi Company for Onshore Operations (ADCO) in conducting this study. The authors acknowledge ADCO and ADNOC management for permission to publish the results of this study.

## References

Bohn, R.B. and Garboczi, E.J., "User Manual for Finite Element Difference Programs: A Parallel Version of NISTIR 6269," National Institute of Standards and Technology Internal Report 6997, (2003).

Grötsch, J. (June 1997): Reservoir Rock Type Scheme for the Upper Thamama Reservoirs: A Basis for the Integrated 3-D Reservoir Characterization Study, *Internal ADCO Report*.

Mavko, G., Mukerji, T., and Dvorkin, J., 2009, Rock Physics Handbook, 2nd Edition, Cambridge University Press

Strohmenger, C. J., L. J. Weber, A. Ghani, K. Al-Mehsin, O. Al-Jeelani, A. Al-Mansoori, T. Al-Dayyani, L. Vaughan, S. A. Khan, and J. C. Mitchell. *Giant Hydrocarbon Reservoirs of the World: From Rocks to Reservoir Characterization and Modeling* AAPG Special Publication Memoir 88 (2006), 139-171.